ACS OMEGA

http://pubs.acs.org/journal/acsodf

Article

Revealing the Mechanisms of Byu dMar 25 in the Treatment of Alzheimer's Disease through Network Pharmacology, Molecular Docking, and In Vivo Experiment

Yikuan Du,[‖] Jinyan Guo,[‖] Yuqi Zhou, Simin Yan, Bijun Xu, Yuni Wang, Duoduo Lu, Zhendong Ma, Qianwen Chen, Qibin Tang, Weichui Zhang, Jinfeng Zhu, Yixing Huang,* and Chun Yang*

Cite This: *ACS Omega* 2023, 8, 25066−25080

Read Online

ACCESS | Metrics & More | Article Recommendations | Supporting Information

ABSTRACT: Background: Alzheimer's disease (AD) is the most common neurodegenerative disease, severely reducing the cognitive level and life quality of patients. Byu dMar 25 (BM25) has been proved to have a therapeutic effect on AD. However, the pharmacological mechanism is still unclear. Therefore, this study aims to reveal the potential mechanism of BM25 affecting AD from the perspective of network pharmacology and experimental validation. Methods: The potential active ingredients of BM25 were obtained from the TCMSP database and literature. Possible targets were predicted using SwissTargetPrediction tools. AD-related genes were identified by using GeneCards, OMIM, DisGeNET, and Drugbank databases. The candidate genes were obtained by extraction of the intersection network. Additionally, the "drug−target−disease" network was constructed by Cytoscape 3.7.2 for visualization. The PPI network was constructed by the STRING database, and the core network modules were filtered by Cytoscape 3.7.2. Enrichment analysis of GO and KEGG was carried out in the Metascape platform. Ledock software was used to dock the critical components with the core target. Furthermore, protein levels were evaluated by immunohistochemistry. Results: In this study, 112 active components, 1112 disease candidate genes, 3084 GO functions, and 277 KEGG pathways were obtained. Molecular docking showed that the effective components of BM25 in treating AD were β-asarone and hydroxysafflor yellow A. The most important targets were APP, PIK3R1, and PIK3CA. Enrichment analysis indicated that the Golgi genetic regulation, peroxidase activity regulation, phosphatidylinositol 3-kinase complex IA, 5-hydroxytryptamine receptor complexes, cancer pathways, and neuroactive ligand−receptor interactions played vital roles against AD. The rat experiment verified that BM25 affected PI3K-Akt pathway activation in AD. Conclusions: This study reveals the mechanism of BM25 in treating AD with network pharmacology, which provides a foundation for further study on the molecular mechanism of AD treatment.

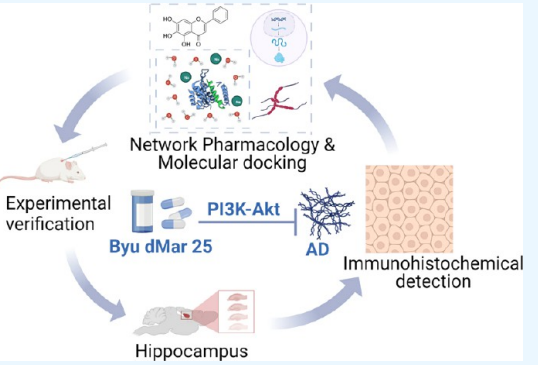

1. INTRODUCTION

Alzheimer's disease (AD) is a degenerative disease of the central nervous system characterized by progressive cognitive impairment. About 50 million people worldwide suffer from AD, and the number is increasing year by year. It is estimated that the number of AD patients will exceed 115 million by 2050.[1] However, the single-target drugs such as galanthamine and memantine used in the clinical treatment of AD can only improve a certain link of AD, with problems such as different curative effects and great toxic and side effects, which cannot improve or even reverse the course of the disease.[2] Currently, there are no specific drugs for AD, and the development of highly effective anti-AD drugs with few side effects has become a hot research topic.

Traditional Chinese medicine (TCM) plays an essential role in the long history of treating AD-related diseases in China. Due to published research confirming the pharmacological effects of TCM and because TCM is relatively safe, cost-effective, and has fewer side effects, TCM treatment has received widespread attention. AD is attributed to the category of "dementia" in Traditional Chinese Medical Science.[3] The disease is situated in the brain, which is related to the deficiency of the liver and kidney, blood-stasis stagnated in an orifice, failure of heart, deficiency, and neurasthenia, and so on.[4] Byu dMar 25 (BM25) is a classic TCM prescription, which is widely used in clinical practice for treating AD. BM25 is composed of 25 kinds of TCM. Among them, coral and safflower are believed to be the principal drugs, which can calm the nerves, promote blood circulation, eliminate fatigue, and relieve menstrual pain; pearl, mother-of-pearl, cinnabar, keel,

Received: March 15, 2023
Accepted: May 25, 2023
Published: June 13, 2023

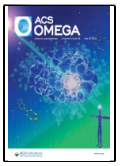

magnet, and brain stone are minister drugs, which have the effects of calming the nerves and tranquilizing liver and yang; Radix Aucklandiae, eaglewood, Aconitum kusnezoffii, Fructus Chebulae, Flos Pyrethri Tatsienensis, and other drugs are assistive drugs, regulating qi-flowing for relieving pain; and *Acorus calamus* L and a small amount of Musk are used as envoy drugs, which can be used for xingnao kaiqiao.[5]

On the whole, the prescription can improve the neurotrophic status and repair neuropathy.[6] Modern medical research has also shown that the main components of BM25 can improve learning and memory ability and have a neuroprotective effect, which shows an excellent curative effect on AD.[7,8] However, BM25 has complex pharmacodynamic components and contains 10 kinds of mineral drugs, which are difficult to dissolve and bring some difficulty to pharmaceutical research, and the pharmacological mechanism of BM25 at the molecular level has been less studied. Therefore, this study aims to systematically investigate the possible mechanism of action of BM25 for the treatment of AD using network pharmacology as well as animal experiments and provide a theoretical basis for expanding the pharmacological action of BM25 and clinical use.

The previous study had preliminarily discussed the pharmacological mechanism of BM25 in treating AD through network pharmacology. It found that the pharmacological mechanism of BM25 against AD may be related to the regulation of MAPK, insulin, mTOR, and other cell signal transduction pathways.[9] However, this study's prediction methods had the space for improvement. In this study, the action mechanism of multicomponent, multitarget, and multipathway of BM25 was further studied by searching the TCMSP database and consulting the literature that reported blood components' identification metabolites of BM25 by UPLC−DAD/Q-TOF-MS,[10] establishing the "drug−target−disease" network. Finally, we used molecular docking technology to verify the results. Our animal experiments also provided an experimental basis, which can provide the pharmacodynamic substance basis and molecular mechanism of BM25 in the treatment of AD. A flowchart of the study design is illustrated in Figure 1.

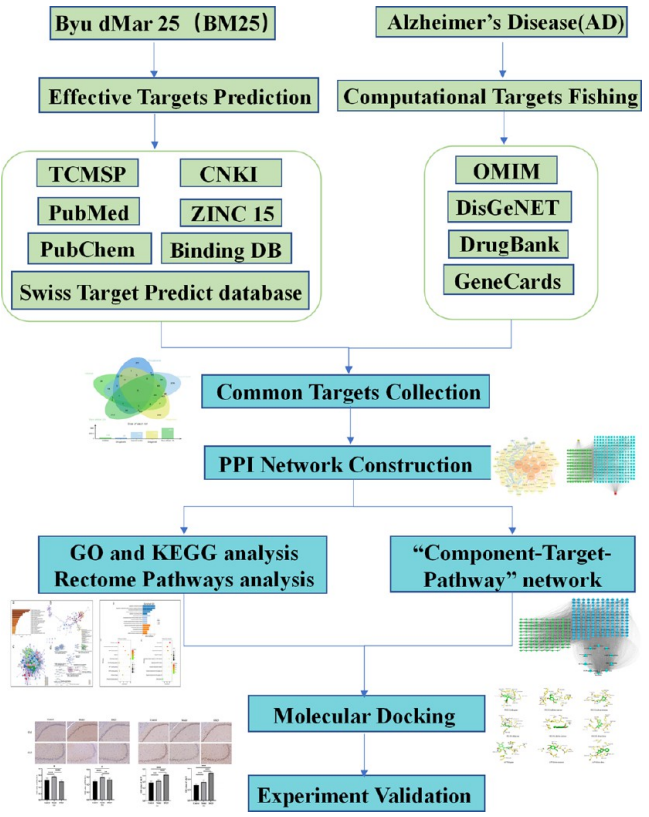

Figure 1. Work flow of the pharmacology-based study of BM25 in the treatment of AD.

2. MATERIALS AND METHODS

2.1. Collection and Screening of Active Components from BM25. The components of the 25 herbs in BM25 were collected from the Traditional Chinese Medicine Systems Pharmacology (TCMSP, http://lsp.nwu.edu.cn/tcmsp.php)[11] (last updated on 2022-08-19). In this study, the active components of BM25 were screened based on pharmacokinetic parameters: absorption, distribution, metabolism, and excretion (ADME).[12] The active components were collected according to oral bioavailability (OB) ≥ 30% and drug-likeness (DL) ≥ 0.18. In addition, the blood−brain barrier (BBB) can be used as an essential index to screen drug information when studying the mechanism of BM25 on nervous system diseases. Therefore, BBB ≥ −0.30 (the molecule is considered to have certain permeability) was used as the screening threshold.[13] Then, we performed a literature study focused on potential active components using PubMed (https://pubmed.ncbi.nlm.nih.gov/) and CNKI (https://www.cnki.net/). By consulting the literature, the active components outside the screening criteria but having explicit biological activity and pharmacological effects were included.

2.2. Prediction of BM25 Targets. The active components and their InChIKey numbers that met the conditions were retrieved from the PubChem database (https://pubchem.ncbi.nlm.nih.gov/)[14] and the Binding DB database (http://www.bindingdb.org/bind/index.jsp). The InChIKey number was converted into SMILES number in the ZINC15 database (http://zinc15.docking.org/).[15] Finally, the collected compound SMILES numbers were imported into the Swiss Target Predict database (http://www.swisstargetprediction.ch/)[16] (last updated on 2022-08-20) for small-molecule protein target prediction. The target information that the "possibility ≥ 0" was obtained.

2.3. Obtaining Related Targets for AD. The AD-related genes were searched by the GeneCards database (http://www.genecards.org/), OMIM database (http://www.omim.org/), DisGeNET database (https://www.disgenet.org/), and Drugbank database (https://www.drugbank.ca/) (last updated on 2022-08-23). All of these databases were comprehensive, freely available online tools and can provide a relatively comprehensive overview of research results. The information of AD-related genes was combined and eliminated the coincident genes by the Jvenn website (https://www.bioinformatics.com.cn).

2.4. Construction of the "Drug−Target−Disease" Network. We used Jvenn to obtain the intersection genes between the drugs and diseases; introduced drug, intersection targets, and disease into Cytoscape 3.7.2 software; and then established the network of "drug−target−disease". In the network, the active drugs, disease, and intersection targets were represented by nodes, and the edges were connected between nodes. The main active components of BM25 in treating

https://doi.org/10.1021/acsomega.3c01683
ACS Omega 2023, 8, 25066−25080

Alzheimer's disease were screened by the node topology eigenvalues "degree" in the network.

2.5. Construction of the "Protein−Protein Interaction" Network. The protein−protein interaction (PPI) network was helpful to discover the vital pharmacophore and utility target of BM25. With the common targets entered into the STRING database (https://string-db.org/),[17] the species origin was defined as "Homo sapiens", the minimum interaction parameter "high confidence (0.90)" was set as the threshold of the core target to construct the PPI network model, and then the TSV format file was downloaded. Afterward, the file information was imported into Cytoscape 3.7.2. by analyzing the network's topological properties through the Network Analyzer plug-in to construct a PPI network based on the node degree and obtain key target proteins.

2.6. Enrichment Analysis of BM25 in Treating AD. Metascape (http://metascape.org/)[18] is a powerful tool for gene function annotation analysis. In this study, Gene Ontology (GO) analysis, Kyoto Encyclopedia of Genes and Genomes (KEGG) signaling pathway analysis, and Reactome analysis were derived from the Metascape database (last updated on 2022-08-26). GO analysis consisted of biological process (BP), cellular component (CC), and molecular function (MF) terms. The top 5 items of GO analysis and the top 10 items of KEGG and Reactome analysis were screened out ($P < 0.01$). The GO analysis chart, KEGG, and Reactome analysis of bubble charts were plotted by using Bioinformatics (http://www.bioinformatics.com.cn/).

2.7. Active Component−Target Molecular Docking. Molecular docking, a tool utilized for the prediction and design of new drugs, can simulate intermolecular combinational patterns between drug ligands and target proteins in 3-dimensional (3D) structures to predict possible docking modes and binding affinities. To validate the compound−target associations, RCSB PDB (http://www.rcsb.org/) was used to retrieve and download the 3D structure files of key target proteins. 3D structure files of compounds were downloaded from PubChem (https://pubchem.ncbi.nlm.nih.gov/). Finally, the Ledock platform[19] was used for molecular docking verification. The results of docking were analyzed by PyMOL. It was generally considered that the numeric value was lower than −5 kJ/mol,[20] indicating that the component had a good binding activity with the target.[21]

2.8. Experimental Verification. *2.8.1. Ethics Statement.* All experimental procedures were conducted in compliance with the National Institutes of Health Guidelines for Care and Use of Laboratory Animals (NIH publications No. 80-23) as revised in 1996 and were approved by the Bioethics Committee of Guangdong Medical University, Dongguan, China.

2.8.2. Animal and Experimental Groups. 18 adult Sprague−Dawley (SD) rats were kept in the Animal Experiment Center of Guangdong Medical University during the experiment, 6 per cage, with 100 mL plastic drinking bottles containing deionized animal drinking water for casual consumption. The mice were randomly divided into 6 in the control group, 6 in the model group, and 6 in the Byu dMar 25 group.

2.8.3. Experimental Drugs and Doses. The drug used in the construction of the aging model was a 30% D-gal solution prepared with saline and injected subcutaneously at a dose of 100 mg/(kg·days). The drug used for gavage was Byu dMar 25, and each capsule (0.5 g) was dissolved in 40 mL of saline to prepare Byu dMar 25 suspension and gavaged at a dose of 64 mg/(kg·days).

2.8.4. Aging Model Construction and Grouping of Animals for Drug Administration. In the model group, 100 mg/(kg·days) D-gal was injected subcutaneously into the back of the neck for 8 weeks, and gavage with saline was started at the 6th week of modeling for 2 weeks. In the Byu dMar 25 group, 100 mg/(kg·days) D-gal was injected subcutaneously into the back of the neck for 8 weeks, and gavage with Byu dMar 25 suspension was started at the 6th week of modeling for 2 weeks. In the control group, saline was injected subcutaneously into the back of the neck for 8 weeks, and gavage with saline was started at the 6th week of modeling for 2 weeks.

2.9. Immunohistochemical Detection. Paraffin-embedded rat brain tissue sections were baked at 65 °C for 60 min, then dewaxed with xylene I and II for 10 min each, and dehydrated with graded concentrations of ethanol for 5 min each. The sections were placed in 50% formamide at 65 °C for 2 h and then washed with sodium citrate buffer solution for five minutes. Subsequently, the sections were treated with 1% H_2O_2 for 5 min, phosphate-buffered saline (PBS) for 10 min, and then washed with PBS three times (10 min each time). The washed sections were added with 5% goat serum/0.3% tritonX-10 and closed for 2 h at room temperature.

The sections were then incubated with anti-AKT2 rabbit pAb and anti-PI3 kinase catalytic subunit alpha/PIK3CA rabbit pAb (both at 1:500 dilution; both from Santa Cruz Biotechnologies, Santa Cruz, CA) at 4 °C overnight. They were then incubated sequentially with respective secondary antibodies (horseradish peroxidase-labeled goat anti-mouse immunoglobulin G [IgG] and horseradish peroxidase-labeled goat anti-rabbit IgG, 1:20 dilution; Sigma Chemical Co.) for 2 h and reacted with avidin-biotinylated horseradish peroxidase and diaminobenzidine (Elite ABC, Vector Laboratories, Burlingame, CA). The sections were rinsed well between steps.

The rinsed sections were added with ready-to-use DAB−H_2O_2 solution for 10 min to avoid light and observe the staining under the microscope. Then, neutral gum was added to seal the sections. For image analysis, five fields were selected randomly from the cross section of each hippocampal area. These fields were photographed at 400 magnification using a computer-based charge-coupled device (CCD) camera system (BX60; Olympus, Tokyo, Japan). Two examiners independently counted and analyzed the hippocampal area number and integrated optical density (IOD) of PIK3CA and AKT in the control and experimental groups in a double-blinded fashion with the aid of a software-based cell counting program (Image-Pro Plus 6.0 software; Media Cybernetics, Inc.). Sections were photographed to collect images of hippocampal area sections.

2.10. Statistical Analysis. GraphPad Prism 9.4.1 software was used for unpaired *t*-test analysis to test the statistical differences between the experimental groups. One-way ANOVA was used for comparison between groups, and the differences were statistically significant ($P < 0.05$) after statistical treatment. All data are expressed as mean ± standard deviation (SD).

3. RESULTS

3.1. Screening of Active Components and Related Targets. A total of 1066 components were found in the TCMSP database. According to the set screening conditions,

https://doi.org/10.1021/acsomega.3c01683
ACS Omega 2023, 8, 25066−25080

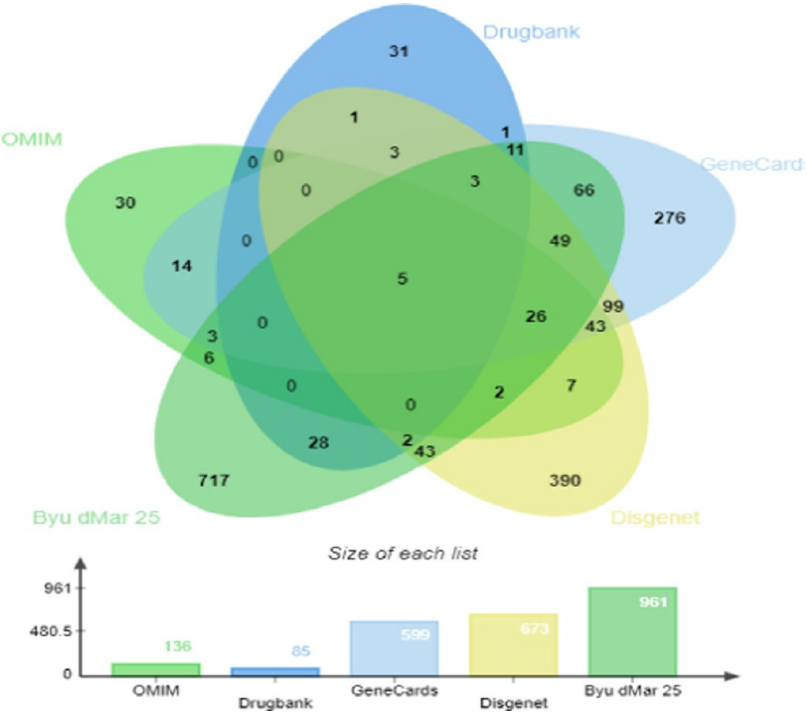

Figure 2. Jvenn diagram of the intersection of the targets of BM25 and AD.

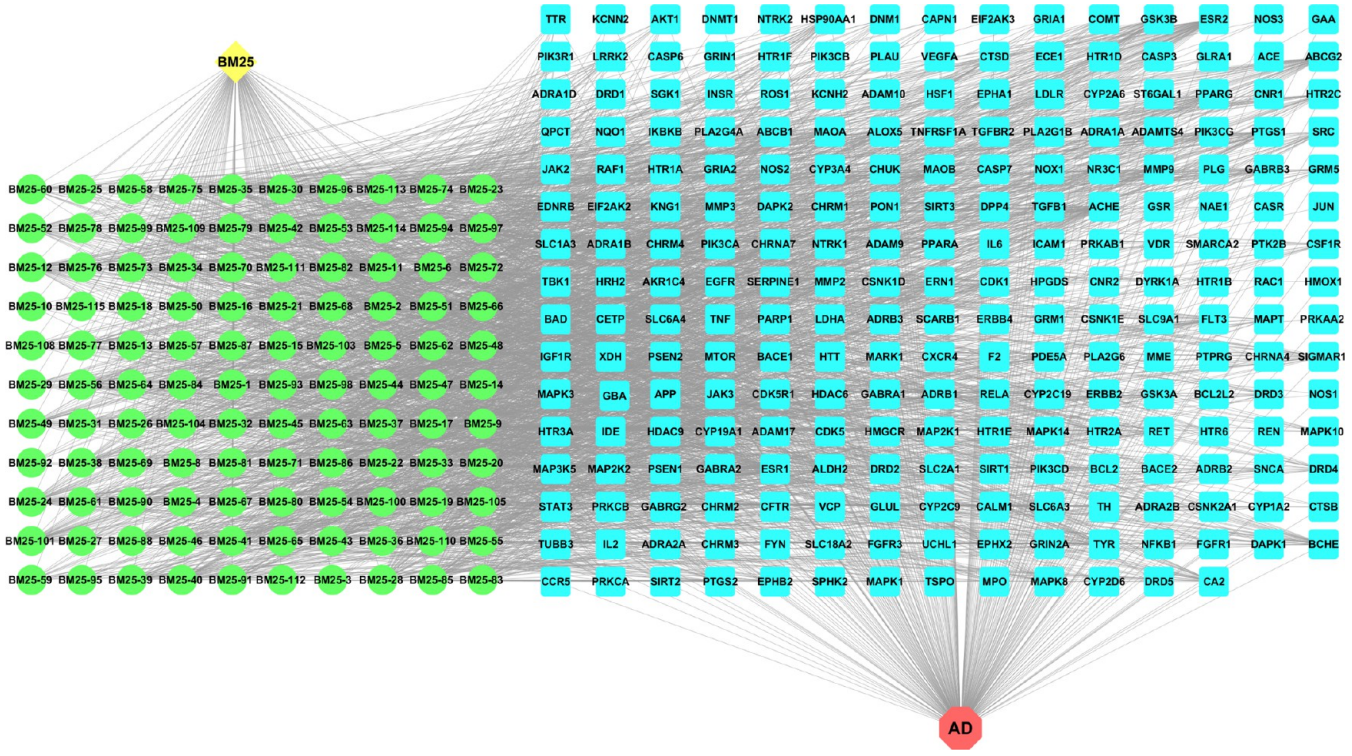

Figure 3. BM25 network diagram of "drug−target−disease".

91 components were selected and supplemented by consulting the literature. Finally, a total of 115 active components were obtained, as shown in Supporting Material 1. Based on the SwissTargetPrediction database's target prediction results, the related targets of BM25 active components were obtained. With "possibility > 0" as the screening condition and then removing repeated targets, a total of 961 targets were obtained.

3.2. Screening of Drug−Disease Intersection Targets.

We obtained 599 targets from the GeneCards database, 136 targets from the OMIM database, 85 targets from the Drugbank database, and 673 targets from the DisGeNET database. After combining four databases, a total of 1112 related gene information were retrieved. Furthermore, the Jvenn diagram was drawn to analyze the target intersection

https://doi.org/10.1021/acsomega.3c01683
ACS Omega 2023, 8, 25066−25080

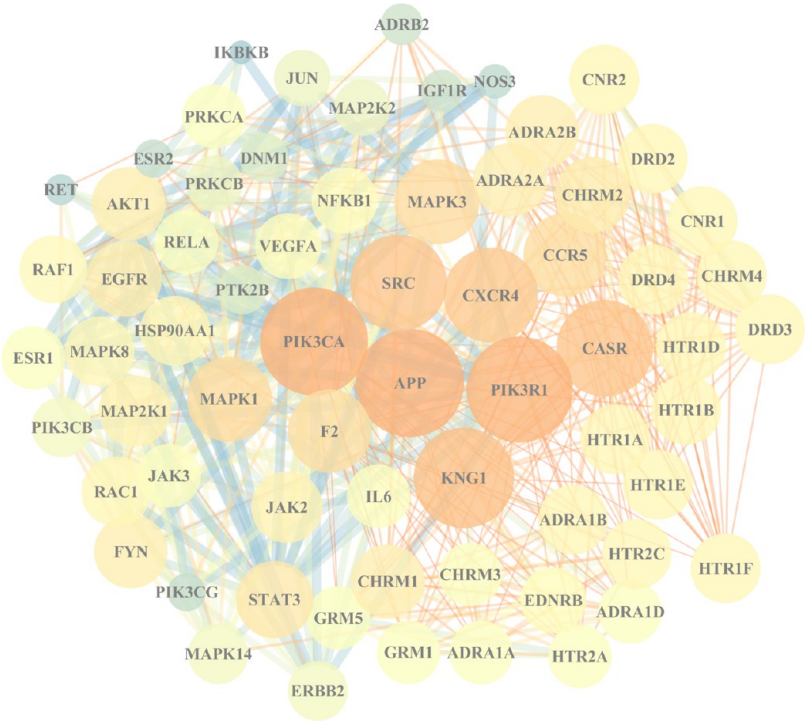

Figure 4. Protein−protein interaction network between BM25 and AD.

between BM25 and AD (Figure 2). We found 238 common targets between BM25 and AD.

3.3. Network Diagram of "Drug−Target−Disease". The network diagram of the "drug−target−disease" of BM25 was constructed using Cytoscape 3.7.2 software (Figure 3). The network graph totally consisted of 350 nodes (including 110 drug nodes and 238 target nodes) and 2833 edges. According to the calculation of the degree size of nodes in the network by Network Analyzer, the top 6 nodes were boldine (degree = 53), norboldine (degree = 50), izoteolin (degree = 47), cheilanthifoline (degree = 46), β-asarone (degree = 44), and 7-acetoxy-2-methyl isoflavone (degree = 43). These key effective molecules with a high degree may play a relatively important role in the pharmacological function of drugs in treating AD.

3.4. Analysis of the "Protein−Protein Interaction" Network. Two hundred thirty-eight intersection targets were uploaded to the STRING database to draw the PPI network, and visual analysis was carried out by Cytoscape 3.7.2 software. The size and color of the nodes were positively correlated with the degree value. The larger the degree value, the larger the node and the darker the color, indicating that the targets were more important in this network relationship. The PPI network (Figure 4) with a threshold of 0.9 was calculated by Cytoscape 3.7.2 software to get the parameter, which finally calculated the BC $\geq$ 0.00364288, CC $\geq$ 0.378119, and degree $\geq$ 28. The core targets APP, PIK3CA, PIK3R1, MAPK1, SRC, MAPK3, KNG1, STAT3, AKT1, and CASR were selected, which were located in the center of the network and had a high overall score, and the previous three were used as molecular docking targets (Table 1). The result that the target of BM25 in treating AD was located in the center suggests that it may play an essential role in the pharmacological action of BM25.

3.5. Functional Pathway Annotation of BM25 Active Components. In this study, a total of 3084 GO entries were enriched by the Metascape database. The first 15 GO entries were selected and plotted according to the minimum *P*-value and biological information ($P < 0.01$) (Figure 5A). The *Y*-axis represented the GO entry, and the area size of the *X*-axis and bar chart represented the number of genes belonging to GO in the target gene set. In the biological process (BP), the common targets were mainly concentrated in the regulation of serotonin secretion, the regulation of dopamine uptake in synaptic transmission, monoterpenes' metabolism, the positive regulation of neuronal maturation, and the regulation of peroxidase activity. In the cellular component (CC), the common targets were mainly concentrated in phosphatidylinositol 3-kinase complex, IA, 5-hydroxytryptamine receptor complex, G-protein-coupled 5-hydroxytryptamine receptor complex, phosphatidylinositol 3-kinase complex, class I, and dopaminergic synapses. In terms of the molecular functional (MF), the common targets were mainly related to dopamine neurotransmitter receptor activity, tetrahydrobiopterin binding, norepinephrine binding, nitric oxide synthase activity, and α1 adrenergic receptor activity.

Table 1. Topological Values of Core Targets in Protein−Protein Interaction Networks

serial number	target	betweenness centrality	closeness centrality	degree
1	APP	0.13045974	0.4746988	53
2	PIK3CA	0.05608386	0.47699758	51
3	PIK3R1	0.05471728	0.47584541	50
4	MAPK1	0.06678717	0.48166259	44
5	SRC	0.05839276	0.47129187	44
6	MAPK3	0.04532395	0.47931873	41
7	KNG1	0.04713192	0.4291939	40
8	STAT3	0.07437091	0.48284314	39
9	AKT1	0.05109262	0.43973214	34
10	CASR	0.01053336	0.40451745	32

https://doi.org/10.1021/acsomega.3c01683
ACS Omega 2023, 8, 25066−25080

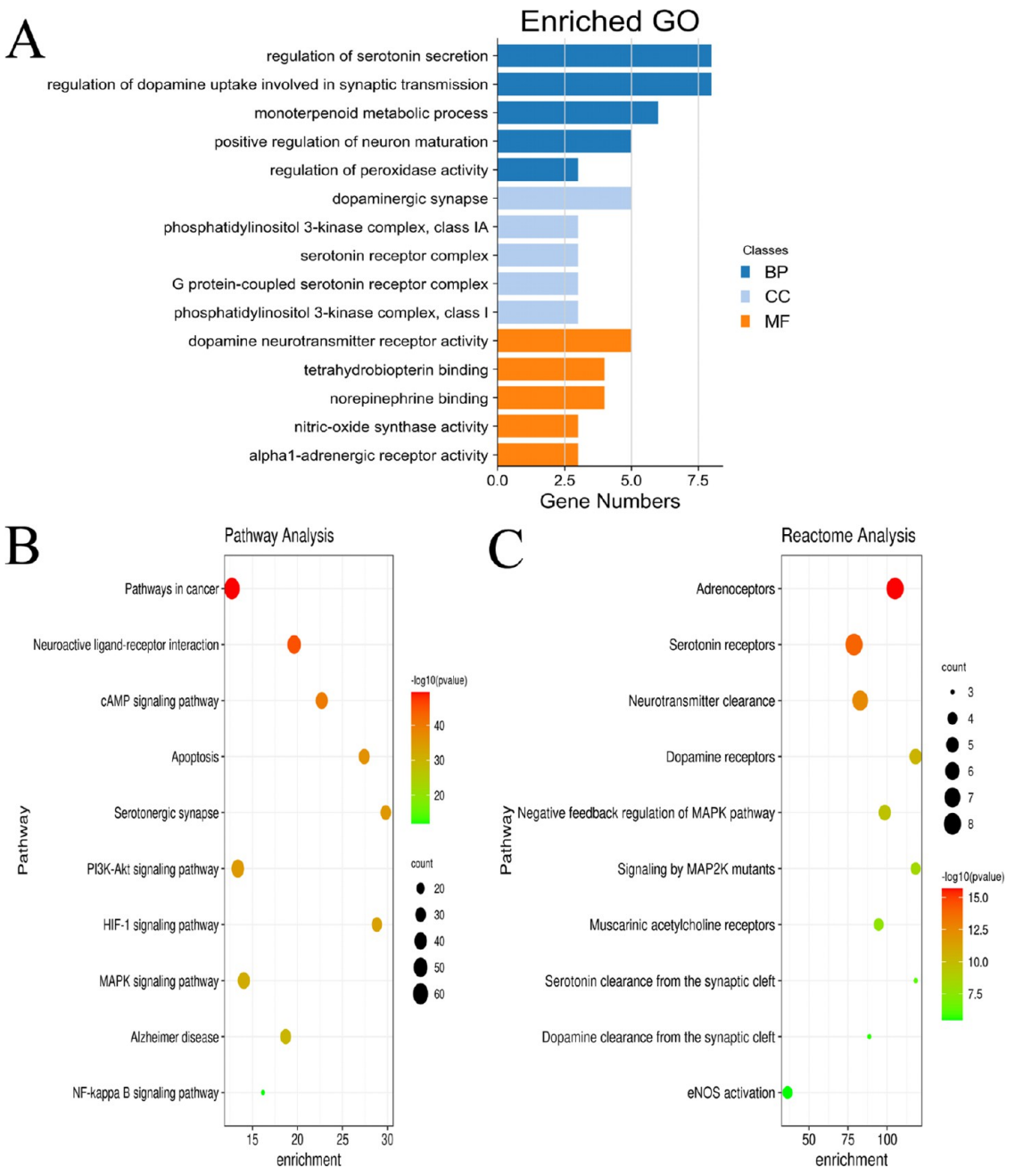

Figure 5. Functional analysis of BM25. (A) Results of GO analysis. (B) Results of KEGG analysis. (C) Results of Reactome analysis.

All of the genes in the KEGG pathway genome had been used as enrichment backgrounds. The collected *P*-value was < 0.01, the minimum count was 3, and the enrichment factor was > 1.5, and they were grouped according to the similarity of their members. More specifically, the *P*-value was calculated based on the cumulative hypergeometric distribution, and the *Q*-value was calculated using the Banjamini−Hochberg process to illustrate multiple tests. A total of 277 enrichment pathways were obtained by KEGG pathway enrichment. The bubble diagram was drawn according to the minimum *P*-value and the first ten biological information pathways combined with biological annotations (Figure 5B). The *Y*-axis represented the name of the pathway. The *X*-axis and bubble area represented the number of genes belonging to this signal pathway in the target gene set. The bubble color represented enrichment significance, that is, the size of the *P*-value. These common targets were enriched in cancer pathways, neuroactive ligand−receptor interactions, cAMP signaling pathways, apoptosis, serotonergic synapses, PI3K-Akt signaling pathways, HIF-1 signaling pathways, MAPK signaling pathways, Alzheimer's disease, and NF- κB signaling pathways.

The screening principle of bubble mapping in Reactome analysis was the same as that of the KEGG pathway. The results showed (Figure 5C) enriched common targets in signal transduction of dopamine receptor, MAP2K mutant, clearance of serotonin from synaptic space, adrenoceptor, negative feedback regulation of MAPK pathway, muscarinic acetylcholine receptor, clearance of dopamine from synaptic space, clearance of neurotransmitters, serotonin receptor, and activation of eNOS.

Interaction enrichment analysis was carried out in STRING 6, BioGrid 7, OmniPath 8, and InWebcast IM 9. The protein−

https://doi.org/10.1021/acsomega.3c01683
ACS Omega 2023, 8, 25066−25080

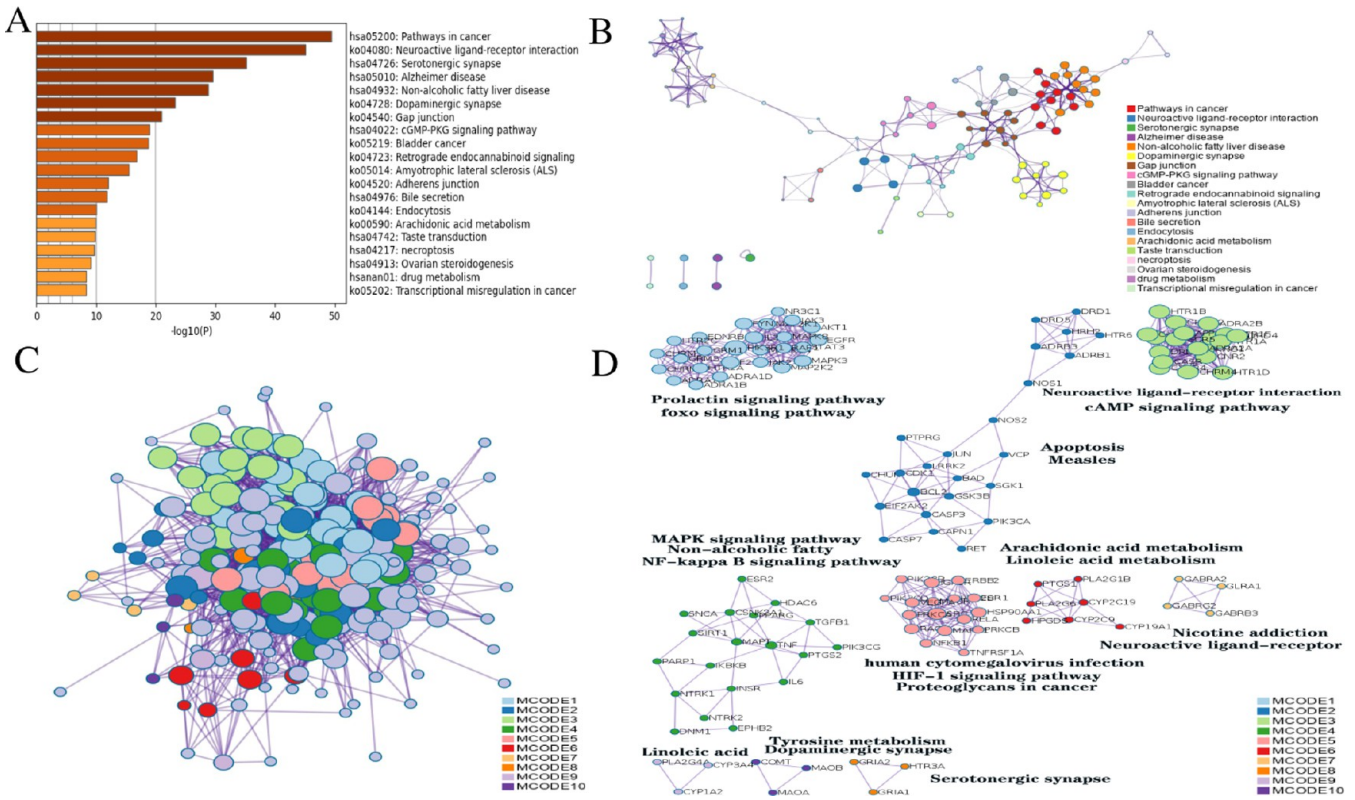

Figure 6. Enrichment network. (A) Metascape showed the main experimental results. (B) Colored by cluster ID, in which the nodes sharing the same cluster ID were usually close to each other. (C) PPI network identified in the gene list. (D) Original MCODE components and functional description.

protein database only used STRING (physical score > 0.132) and physical interactions in BioGrid. The resulting network contained a subset of proteins that form a physical interaction with at least one other member of the list. If the network contained 3−500 proteins, the molecular complex detection (MCODE) algorithm 10 had been applied to identify densely connected network components. The MCODE network identified for a single gene list had been collected (Figure 6). Path and process enrichment analysis had been applied to each MCODE component. The three best score items by the *P*-value were retained as functional descriptions of the corresponding components (Table 2).

Using the analysis of this series of practical tests, we can provide valuable information to explain the possible mechanism of BM25 in treating AD.

3.6. Results of the "Component−Target−Pathway" Network. The BM25 "Component−Target−Pathway" network was constructed using Cytoscape 3.7.2 with 115 drug components, 238 intersection targets, and 10 crucial pathways (Figure 7). The network diagram was composed of components, targets, and signal pathways; the green lozenges represent the drugs; the blue octagons represent the targets; and sky blue rotundities represent the signal pathways. According to the edge area, the first three components were selected for molecular docking verification, which were *β*-asarone, lignan, and baicalein.

3.7. Results of BM25 Core Component−Target Molecule Docking. The 3 core targets with a high score in PPI were docked with the core components of BM25 (Figure 8). It was generally believed that a score of less than −5 kJ/mol indicated a good binding activity between the compound and the target. The molecular docking results showed that the score of lignans, baicalein, and *β*-asarone with APP, PIK3R1, and PIK3CA were less than −5 kJ/mol (Table 3), indicating that the core compounds had a good bonding activity with core targets.

Table 2. Functional Description of the Corresponding Components of the Three Best Score Items by the *P*-Value

MCODE	GO	description	Log 10(*P*)
MCODE1	hsa04917	prolactin signaling pathway	−19.2
MCODE1	hsa04068	foxo signaling pathway	−18.8
MCODE2	hsa04210	apoptosis	−12.4
MCODE2	hsa05162	measles	−12.2
MCODE3	hsa04080	neuroactive ligand−receptor interaction	−24.7
MCODE3	ko04024	cAMP signaling pathway	−10.4
MCODE4	hsa04010	MAPK signaling pathway	−10.8
MCODE4	hsa04932	non-alcoholic fatty liver disease	−9
MCODE4	ko04064	NF-kappa B signaling pathway	−8.4
MCODE5	hsa05163	human cytomegalovirus infection	−23.7
MCODE5	hsa04066	HIF-1 signaling pathway	−22.2
MCODE5	ko05205	proteoglycans in cancer	−22.1
MCODE6	hsa00590	arachidonic acid metabolism	−15.2
MCODE6	hsa00591	linoleic acid metabolism	−10.5
MCODE7	ko04080	neuroactive ligand−receptor interaction	−8
MCODE7	hsa05033	nicotine addiction	−7.9
MCODE8	hsa04726	serotonergic synapse	−8.9
MCODE9	hsa00591	linoleic acid metabolism	−9
MCODE10	hsa00350	tyrosine metabolism	−8.4
MCODE10	ko04728	dopaminergic synapse	−7

https://doi.org/10.1021/acsomega.3c01683
ACS Omega 2023, 8, 25066−25080

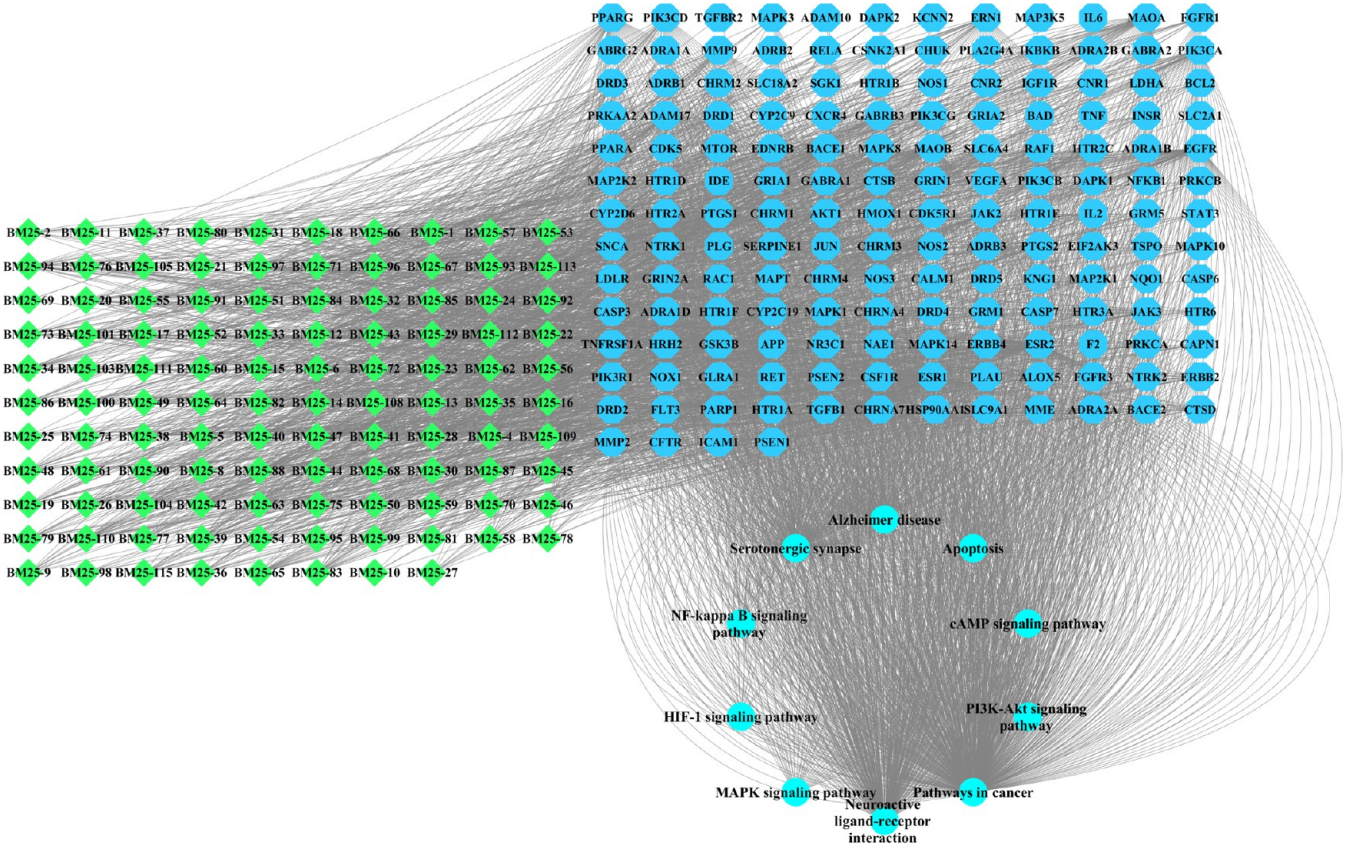

Figure 7. "Component−Target−Pathway" network diagram.

3.8. Effect of BM25 on Hippocampus of SD Rats with the D-Gal Aging Model. In order to verify the reliability of the main active ingredients for treating AD, this experiment established an AD rat model, used the suspension of BM25 with the concentration of 64 mg/(kg·days) for animal experiments, and took photos to collect the cross-sectional images of hippocampus in the immunohistochemical staining results. The results showed that, compared with the control group, AKT positive staining expression in CA1 and CA3 areas of the hippocampus of SD rats in the model group and BM25 group increased significantly. Compared with the model group, the AKT positive staining expression in hippocampal CA1 and CA3 areas of SD rats in the BM25 group also increased significantly (Figure 9, $P < 0.05$). In addition, compared with the control group, the expression of PIK3CA in hippocampal CA1 and CA3 of SD rats in the model group increased significantly, while the positive staining expression of PIK3CA in hippocampal CA1 and CA3 of SD rats in the BM25 group decreased significantly compared with the model group (Figure 10, $P < 0.05$).

4. DISCUSSION

Alzheimer's disease is a neurodegenerative disease with progressive deterioration of cholinergic neurons, characterized by extracellular β-amyloid and hyperphosphorylated t-protein, which are a significant component of neurofibrillary tangles and neuroinflammation.[22] AD poses a severe threat to the health of the world's elderly population. At present, the targets of drug therapy are mainly based on Aβ toxicity and abnormal tau hyperphosphorylation. Further research and development are complex.[23] TCM can not only interfere with the above two targets to treat AD but also effectively interfere with AD by regulating potential targets such as autophagy, brain−gut axis, and interstitial fluid in the brain, which shows great potential in the treatment of AD.[24] BM25 is a classic prescription of traditional Tibetan medicine, commonly used in neurological diseases.[25] Studies[26] have shown that 25 flavored coral pills can treat Alzheimer's disease by regulating intestinal flora; however, its specific mechanism and pathway are not precise. In this paper, the process of BM25 in treating AD was studied by network pharmacology, and its mechanism was further revealed.

This study found that the main active components of BM25 include lignans, baicalein, β-asarone, and so on. Previous studies showed that long-term oral administration of baicalein inhibited the activities of lipoxygenase and glycogen synthase kinase 3β (GSK3β) in the hippocampus of APP/PS1 mice, decreased the total concentration of Aβ, and prevented tau phosphorylation.[27] β-Asarone can also inhibit the phosphorylation level of GSK3β in treating AD.[28] Studies have shown that baicalein and β-asarone, components of BM25, can play a therapeutic role in other diseases of the human body by inhibiting the PI3K-AKT signaling pathway. This study verified that BM25 can treat the cognitive impairment of aging rats by inhibiting the PI3K-AKT signaling pathway. At the same time, in the "drug−disease−target" network diagram of this study, the degree values of lignans, baicalein, and β-asarone are high, and they are related to more than 10 genes. Therefore, we speculate that the main components that play a role in BM25 may be lignans, baicalein, β-asarone, and so on. This provides a basis for studying the therapeutic effect of BM25 on AD from the level of practical monomer components.

https://doi.org/10.1021/acsomega.3c01683
ACS Omega 2023, 8, 25066−25080

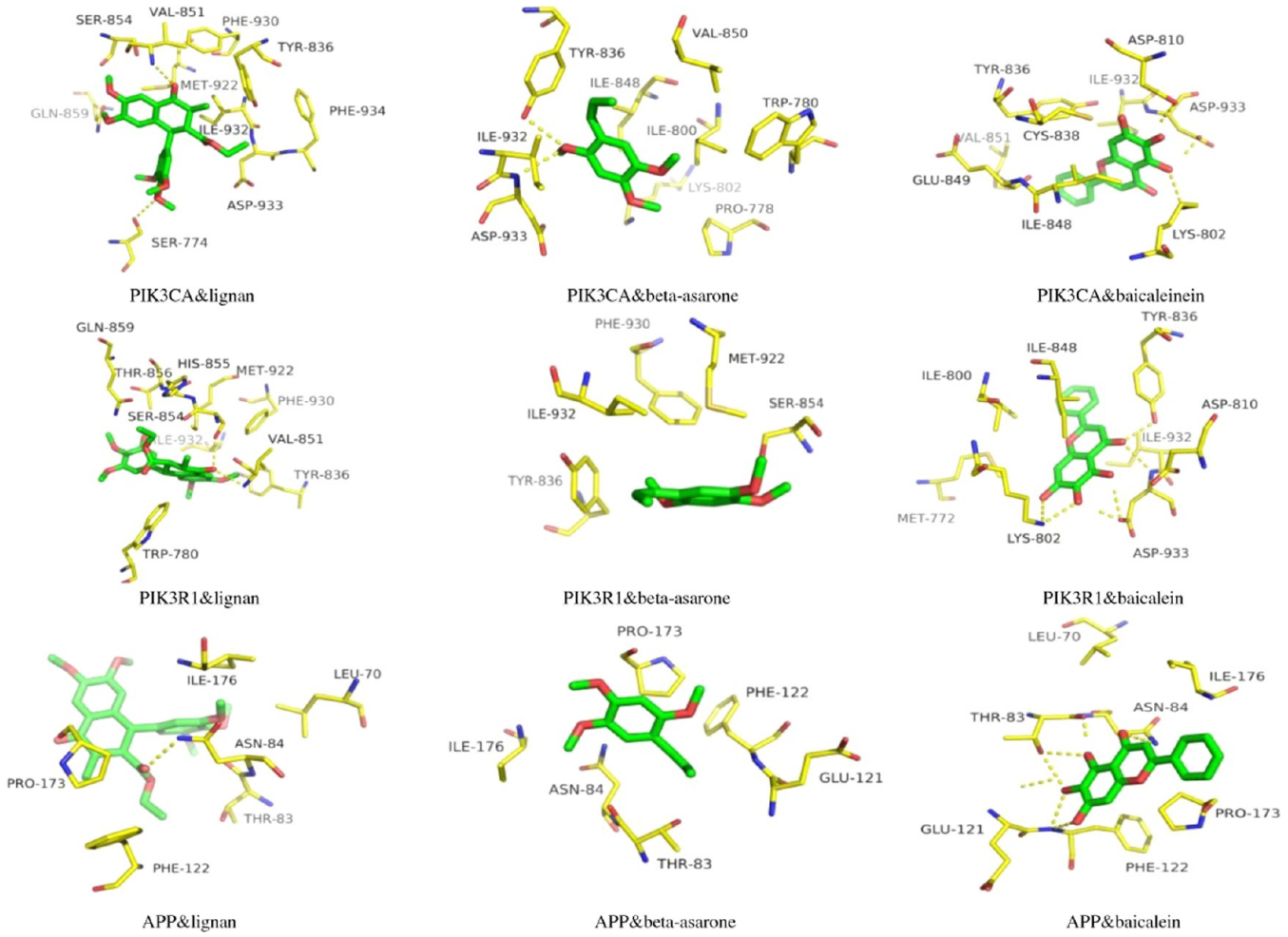

Figure 8. Molecular docking diagram.

Table 3. Molecular Docking Score Table

target	component	score
PIK3CA	lignan	−27.6716 kJ/mol
	baicalein	−26.1668 kJ/mol
	β-asarone	−15.2152 kJ/mol
PIK3R1	lignan	−27.7552 kJ/mol
	baicalein	−26.2086 kJ/mol
	β-asarone	−16.0512 kJ/mol
APP	lignan	−15.9676 kJ/mol
	baicalein	−17.9322 kJ/mol
	β-asarone	−11.913 kJ/mol

In this study, through PPI analysis, it is found that APP, PIK3CA, PIK3R1, AKT1, and other targets are the core targets of BM25 in treating AD. Amyloid precursor protein (APP) is a transmembrane protein. In organisms, APP is cut by *β* secretase and *γ* secretase to produce *β*,[29] which is normally produced and degraded to maintain balance. By inhibiting the production of APP, the deposition of A*β* in the brain can be reduced.[30] Studies have shown that APP gene mutation is the basis of A*β* deposition.[31] PIK3CA is a member of the phosphatidylinositol 3-kinase (PI3K) protein family, a catalytic subunit of PI3K,[32] and a key downstream protein kinase of PI3K/Akt/mTOR signaling pathway, which plays an essential role in catabolism, cell adhesion, and apoptosis.[33] AKT1 gene encodes AKT serine/threonine kinase 1, and AKT1 protein plays a wide range of cellular functions in neuronal survival. And it has been proved to be involved in tau phosphorylation, which may be related to AD and other neurodegeneration.[34] Studies have shown that ROS-mediated oxidative modification of AKT1 can lead to synaptic dysfunction in AD, and AKT1 can mediate A*β*42 to cause cognitive impairment in rats and mice.[35] According to the data of this study, APP, PIK3CA, PIK3R1, AKT1, and other targets are enriched in the PI3K-AKT1 signaling pathway, which indicates that this pathway has a rich research value.

In this study, the "composition−target−signal pathway" diagram was drawn to describe the mechanism of BM25 in treating AD as a whole (Figure 7), and the top 10 signal pathways with rich degrees were selected to show the most possible pathways, such as the PI3K-AKT pathway, NF-*κ*B pathway, cancer pathway, etc. In the brain, the PI3K/Akt signaling pathway has a wide range of functions: regulating survival, cell proliferation, growth, differentiation, movement, intracellular transport, the extension of neurites (dendrites and axons), and so on.[36,37] PI3K transmits the receptor tyrosine kinase signal to survival kinase AKT through phosphatidylinositol 3,4,5-triphosphate (PIP3). The increase of the PIP3 level on the membrane will lead to the colocation of proteins (such as AKT and PDK1) containing the pleckstrin homology (PH) domain, which will lead to kinase-mediated phosphorylation and activation.[38] The PI3K/Akt signaling pathway is one of the critical axes to support the synaptic plasticity of neurons. By

https://doi.org/10.1021/acsomega.3c01683
ACS Omega 2023, 8, 25066−25080

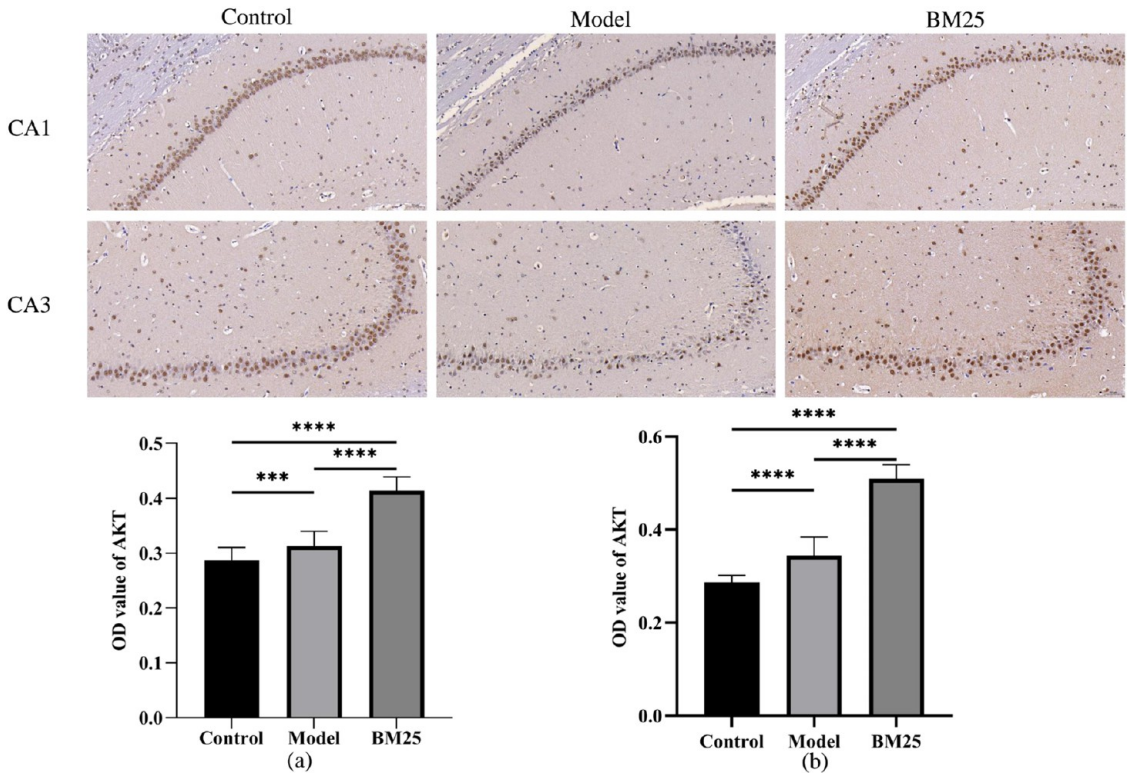

Figure 9. Effect of BM25 on the expression of AKT in brain tissues of brain aging mice. (a) OD value of AKT in CA1. (b) OD value of AKT in CA3 (***$P < 0.001$; ****$P < 0.0001$).

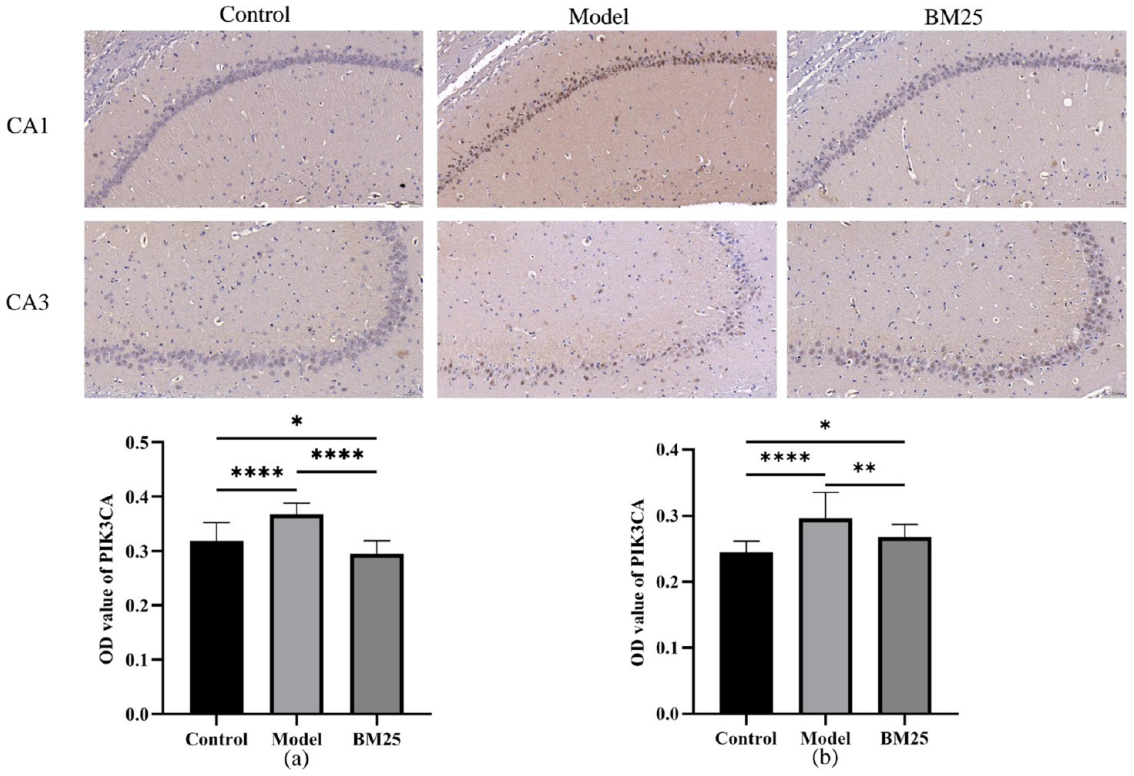

Figure 10. Effect of BM25 on the expression of PIK3CA in brain tissues of brain aging mice. (a) OD value of PIK3CA in CA1. (b) OD value of PIK3CA in CA3 (*$P < 0.05$; **$P < 0.01$; ***$P < 0.001$; ****$P < 0.0001$).

maintaining the survival of nerve cells, controlling the phosphorylation mode of tau protein, and regulating the clearance of Aβ, oxidative stress and excessive production of ROS can stimulate the PI3K/Akt signaling pathway in nerve cells to increase the production of Aβ plaques.[39] The researchers found that the mTOR pathway is significant in

https://doi.org/10.1021/acsomega.3c01683
ACS Omega 2023, 8, 25066−25080

the regulation of autophagy, and the activity of mTOR is significantly regulated by the PI3K/Akt pathway, while the PI3K/Akt pathway is overactive in patients with cognitive impairment or AD.[40] Heras-Sandoval and others also found that the upregulation of the PI3K/Akt/mTOR pathway is closely related to the clearance of Aβ and tau proteins, synaptic loss, and cognitive decline in AD patients.[41] Investigation[42] on the state of the PI3K/Akt system in the brain of individuals with AD shows that the abnormal and continuous activation of PI3K/Akt/mTOR signal transduction of neurons is the early feature of the disease. In the case of synaptic transmission defect that leads to cognitive decline, the increase of activation of the PI3K/Akt/mTOR axis of neurons is the main candidate effect system for transmitting pathophysiological signals from Aβ to tau.[42] Studies have shown that bleomycin can significantly eliminate Aβ in microglia and primary neurons by inhibiting autophagy induced by the PI3K-AKT pathway.[43] Curcumin inhibits the production of Aβ and induces autophagy by downregulating the PI3K/Akt/mTOR signaling pathway, further showing a neuroprotective effect.[44] Studies[45] have shown that oregano sapogenin can increase the phosphorylation level of GSK3β (Ser9), inhibit the activation of PI3K/Akt, increase the phosphorylation level of PI3P85 and Akt Ser 473, and weaken the hyperphosphorylation of tau induced by Aβ through the PI3K/Akt/GSK3β cascade. Based on the above research, it can be seen that the purpose of treating AD can be achieved by inhibiting the PI3K-AKT signaling pathway.

The existing research shows that abnormal neural network activity, synapse reduction, and abnormal function and the degeneration of neurons in specific parts are the main reasons for the cognitive decline of AD patients.[46] Regarding AD, oligomers and multimers formed by Aβ and apoptotic neuronal cell fragments can activate immune cells in the brain microglia and astrocytes through toll-like receptors or advanced glycation end product receptors and then trigger local chronic inflammatory reactions.[47] For neuroinflammation in the pathogenesis of AD, microglia and astrocytes are the main sources of cytokines in the neuroinflammation of AD. It has been proved that Aβ can activate the complement system and microglia, leading to the release of allergic toxins and proinflammatory cytokines further to promote inflammation.[48] The brain inflammatory cascade mediated by microglia and cytokines is the basis of the pathogenesis of AD, some studies have described the central role of proinflammatory cytokines such as tumor necrosis factor-α (TNF-α) and interleukin (such as IL-1, IL-1β, IL-6) in the pathophysiology of AD, including mild cognitive impairment (MCI) to comprehensive late stage.[49] MiR-107 was proven to reduce the expression level of FGF7, inactivate the FGFR2/PI3K/Akt pathway, and improve the inflammation and apoptosis of SH-SY5Y cells induced by Aβ.[50] Studies have shown that the inflammatory reaction induced by endotoxin can be alleviated by inhibiting the PI3K/AKT/IκB/NFκB signaling pathway,[51] and the TLR4 activated on LPS-induced neuroinflammation microglia can recruit the PI3K/AKT signaling axis to improve the nuclear translocation of inflammatory transcription factor NF-κ B and enhance the expression of genes encoding inflammatory cytokines (TNF-α and IL-1-β) and proteins (COX-1, COX-2, and iNOS).[52] The destructive effects of these mediators on neuron survival and mitochondrial function may disrupt synaptic connections, leading to brain atrophy and cognitive decline. In addition, due to the dysfunction of microglia mitochondria, reactive oxygen species (ROS) and iNOS synergistically reactivate NF-κB to enhance the inflammatory response, which leads to neurodegeneration, neuronal damage, and neuronal cell death.[52,53] Studies have shown that inhibiting the PI3K/Akt signaling pathway improves cognitive impairment, reduces neuronal damage, and inhibits the activation of astrocytes in the hippocampus of AD.[54]

Liu et al.[55] found that BM25 can reduce the activity of human neuroblastoma cell SHSY-5Y through the NF-κB pathway and inhibit the process of cell proliferation, which is mutually confirmed with the signal pathway of NF-κB in KEGG analysis and the process of cell proliferation in GO analysis. This study shows that BM25 can treat AD by acting on the corresponding GO process, such as the regulation of peroxidase activity, which can catalyze many reactions. Catalase is one of the key antioxidant enzymes, which can reduce oxidative stress to a great extent by destroying cell hydrogen peroxide to produce water and oxygen. The lack or dysfunction of catalase is considered to be related to the pathogenesis of many age-related degenerative diseases.[56] Oxidative stress participates in the development of AD by promoting the deposition of Aβ, hyperphosphorylation of tau, and subsequent loss of synapses and neurons.[57] In oxidative stress, ROS recruited the PI3K/Akt signaling pathway to reduce the expression of heat shock factor-1 (HSF-1) in nerve cells, thus reducing the expression of heat shock protein-70 and crystallin, which led to excessive accumulation of the Aβ oligomer.[58]

Du et al.[59] observed the effects of BM25 on the neurotransmitter NO and nitric oxide synthase (NOS) in the plasma of mice with peripheral and central pain and migraine rats and found that BM25 could reduce the contents of NO and NOS in the plasma of migraine rats, which was consistent with the results of Reactome analysis, as shown in Figure 5C. There are many experimental studies on the pharmacological mechanism of BM25 in signal pathways. The results show that dopamine receptor response is the most significant, and dopamine analogues have been reported to have significant biological activities in the treatment of Parkinson's disease and Alzheimer's disease, suggesting that BM25 may treat AD through the dopamine receptor response pathway.[60] We use Metascrape software to build a rich terminology network (Figure 6B), which is colored by cluster ID, in which nodes sharing the same cluster ID are usually close to each other and decomposed into 20 densely linked topological modules, among which the prolactin signal pathway, as the largest signal pathway of Log 10(P), has been found in recent years[61] to be a key molecule involved in the early events and the late stages of Alzheimer's disease. This paper provides molecular evidence for a further study of prolactin through modular analysis.

The above analysis shows that BM25 can treat AD through multicomponents, multichannels, and multitargets, among which the PI3K/Akt pathway is highly correlated with BM25 in treating AD. In addition, the docking results of the BM25 core component−target molecule in this paper show that there is good binding activity between the component and target, which also verifies the results in network analysis to some extent. At the same time, the score of our molecular docking was less than −25 kJ/mol in five cases, and the binding activity between lignans and APP was the strongest. And the component also performed well in the protein−protein interaction network, suggesting a new research point of the BM25 active component in the treatment of AD. However, the

https://doi.org/10.1021/acsomega.3c01683
ACS Omega 2023, 8, 25066−25080

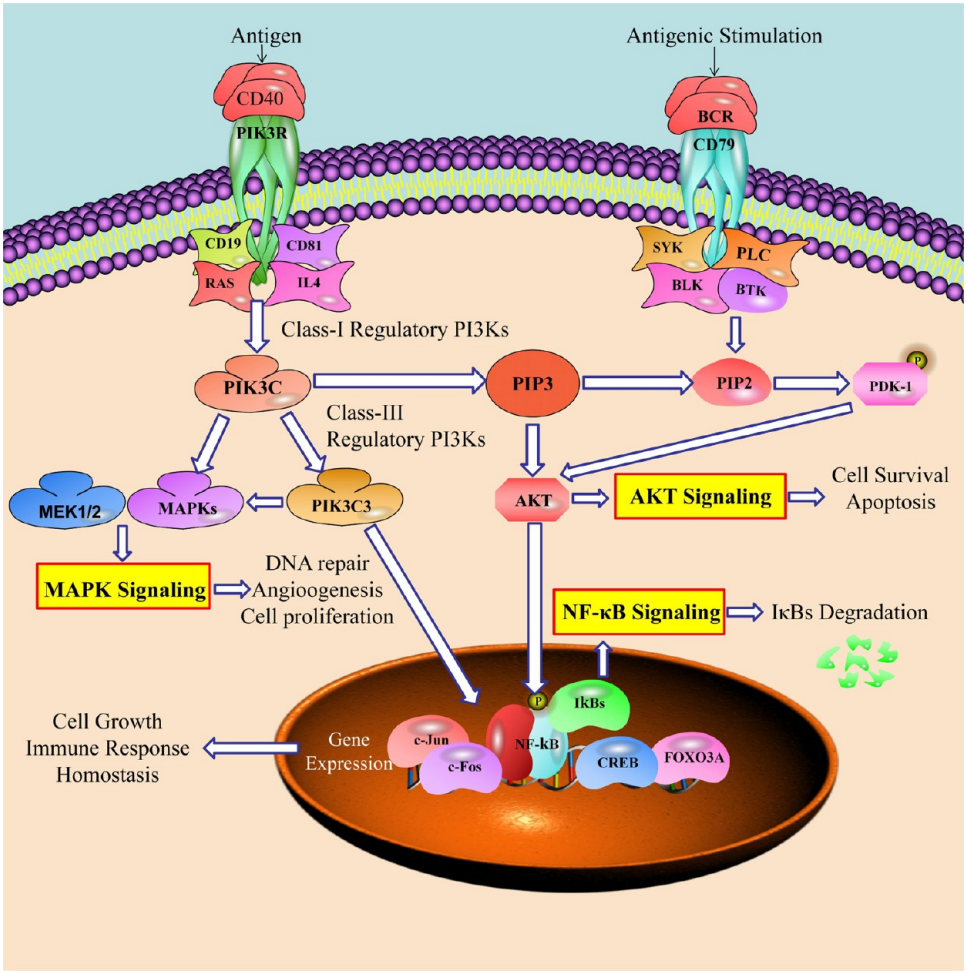

Figure 11. Scientific hypothesis diagram.

molecular docking score of glycyrrhizin A, an important component of BM25, is low with the core target, but there are related clinical treatments in the literature, which suggests that our target at the edge of PPI network analysis also has research prospects. Through the immunohistochemical study on hippocampus of aging rats, we found that, compared with the control group, the protein expressions of PIK3CA and AKT in the model group increased. At the same time, compared with the model group, PIK3CA in the hippocampus of the BM25 group decreased and AKT expression increased. This may be due to the increase of oxidative stress and inflammatory reaction in aging rats, which stimulated the PI3K/Akt signaling pathway of nerve cells and then activated mTOR phosphorylation,[62] which led to the activation of microglia, thus increasing the release of inflammatory cytokines.[63] In addition, mTOR inhibits autophagy, leading to amyloid β-protein deposition and neurodegeneration, which leads to brain atrophy and cognitive decline. Therefore, BM25 may improve AD by regulating the PI3K/AKT signaling pathway and reducing the production of Aβ plaque. In the early drug experiment of aging rats, we found that BM25 has a protective effect on the nervous system. In the further study, the research group predicted that β-asarone and hydroxysafflor yellow A were the active ingredients, APP, PIK3CA, PIK3R1, and AKT1 were the targets, and the PI3K/Akt pathway and 5-hydroxytryptamine synaptic pathway were the breakthrough points. On this basis, we drew a scientific hypothesis diagram (Figure 11). It provided a foundation for a comprehensive and in-depth understanding of the molecular mechanism.

5. CONCLUSIONS

Although the efficacy of BM25 in treating AD has been confirmed by many studies, the molecular mechanisms of BM25 still remain unclear. In the study, we screened 115 major active components and 238 major targets. The mechanisms employed by BM25 against AD were related to 277 signaling pathways, especially the PI3K/Akt pathway. Lastly, we used molecular docking methods to evaluate the binding activity between the targets and active components of BM25. The binding activity between lignans and PIK3R1 was the strongest. This study provided a systematic view of the potential mechanisms against AD.

■ ASSOCIATED CONTENT

Data Availability Statement

All data are fully available without restriction, and all relevant data are included within the paper.

Supporting Information

The Supporting Information is available free of charge at https://pubs.acs.org/doi/10.1021/acsomega.3c01683.

Information of 115 active components screened from BM25 (Table S1) and list of abbreviations (Table S2) (PDF)

https://doi.org/10.1021/acsomega.3c01683
ACS Omega 2023, 8, 25066−25080

AUTHOR INFORMATION

Corresponding Authors

Yixing Huang − *Dongguan Key Laboratory of Chronic Inflammatory Diseases, The First Dongguan Affiliated Hospital, Guangdong Medical University, Dongguan 523000, China; Dongguan Key Laboratory of stem cell and regenerative tissue engineering, Guangdong Medical University, Dongguan 523808, China;* Email: huangyixing1028@163.com

Chun Yang − *Dongguan Key Laboratory of Chronic Inflammatory Diseases, The First Dongguan Affiliated Hospital, Guangdong Medical University, Dongguan 523000, China; Dongguan Key Laboratory of stem cell and regenerative tissue engineering, Guangdong Medical University, Dongguan 523808, China;* orcid.org/0000-0001-5813-0914; Email: yangchunangel@163.com

Authors

Yikuan Du − *Central Laboratory, The Tenth Affiliated Hospital of Southern Medical University, Dongguan 523059, China;* orcid.org/0000-0001-9568-0907

Jinyan Guo − *Dongguan Key Laboratory of Chronic Inflammatory Diseases, The First Dongguan Affiliated Hospital, Guangdong Medical University, Dongguan 523000, China; Dongguan Key Laboratory of stem cell and regenerative tissue engineering, Guangdong Medical University, Dongguan 523808, China;* orcid.org/0000-0002-8561-3054

Yuqi Zhou − *Dongguan Key Laboratory of Chronic Inflammatory Diseases, The First Dongguan Affiliated Hospital, Guangdong Medical University, Dongguan 523000, China; Dongguan Key Laboratory of stem cell and regenerative tissue engineering, Guangdong Medical University, Dongguan 523808, China*

Simin Yan − *Dongguan Key Laboratory of Chronic Inflammatory Diseases, The First Dongguan Affiliated Hospital, Guangdong Medical University, Dongguan 523000, China; Dongguan Key Laboratory of stem cell and regenerative tissue engineering, Guangdong Medical University, Dongguan 523808, China;* orcid.org/0000-0003-3061-7610

Bijun Xu − *Dongguan Key Laboratory of Chronic Inflammatory Diseases, The First Dongguan Affiliated Hospital, Guangdong Medical University, Dongguan 523000, China; Dongguan Key Laboratory of stem cell and regenerative tissue engineering, Guangdong Medical University, Dongguan 523808, China;* orcid.org/0000-0001-9475-6156

Yuni Wang − *Dongguan Key Laboratory of Chronic Inflammatory Diseases, The First Dongguan Affiliated Hospital, Guangdong Medical University, Dongguan 523000, China; Dongguan Key Laboratory of stem cell and regenerative tissue engineering, Guangdong Medical University, Dongguan 523808, China;* orcid.org/0000-0001-6039-5380

Duoduo Lu − *Dongguan Key Laboratory of Chronic Inflammatory Diseases, The First Dongguan Affiliated Hospital, Guangdong Medical University, Dongguan 523000, China; Dongguan Key Laboratory of stem cell and regenerative tissue engineering, Guangdong Medical University, Dongguan 523808, China;* orcid.org/0009-0000-2806-2674

Zhendong Ma − *Dongguan Key Laboratory of Chronic Inflammatory Diseases, The First Dongguan Affiliated Hospital, Guangdong Medical University, Dongguan 523000, China; Dongguan Key Laboratory of stem cell and regenerative tissue engineering, Guangdong Medical University, Dongguan 523808, China;* orcid.org/0000-0002-2180-9381

Qianwen Chen − *Dongguan Key Laboratory of Chronic Inflammatory Diseases, The First Dongguan Affiliated Hospital, Guangdong Medical University, Dongguan 523000, China; Dongguan Key Laboratory of stem cell and regenerative tissue engineering, Guangdong Medical University, Dongguan 523808, China;* orcid.org/0000-0001-9629-9833

Qibin Tang − *Dongguan Key Laboratory of Chronic Inflammatory Diseases, The First Dongguan Affiliated Hospital, Guangdong Medical University, Dongguan 523000, China; Dongguan Key Laboratory of stem cell and regenerative tissue engineering, Guangdong Medical University, Dongguan 523808, China;* orcid.org/0000-0002-9777-1949

Weichui Zhang − *Dongguan Key Laboratory of Chronic Inflammatory Diseases, The First Dongguan Affiliated Hospital, Guangdong Medical University, Dongguan 523000, China; Dongguan Key Laboratory of stem cell and regenerative tissue engineering, Guangdong Medical University, Dongguan 523808, China;* orcid.org/0000-0001-8501-3588

Jinfeng Zhu − *Dongguan Key Laboratory of Chronic Inflammatory Diseases, The First Dongguan Affiliated Hospital, Guangdong Medical University, Dongguan 523000, China; Dongguan Key Laboratory of stem cell and regenerative tissue engineering, Guangdong Medical University, Dongguan 523808, China;* orcid.org/0000-0002-1737-0185

Complete contact information is available at: https://pubs.acs.org/10.1021/acsomega.3c01683

Author Contributions

[‖]Y.D. and J.G. contributed equally to this study and share first authorship. Y.D. and J.G. conceived the study and contributed equally to this study. S.Y., B.X., D.L., and Y.W. edited the manuscript. Z.M. and Q.C. analyzed the data. Q.T., Y.Z., W.Z., and J.Z. were responsible for figure drawing and table design. Y.H. and C.Y. revised the manuscript. All authors have read and approved the final manuscript.

Notes

The authors declare no competing financial interest.

ACKNOWLEDGMENTS

This work was supported by the Natural Science Foundation of Guangdong Province (Nos. 2021A1515011580, 2021B1515140012, and 2023A1515010083), Dongguan Science and Technology of Social Development Program (No. 20211800905342), the Administration of Traditional Chinese Medicine of Guangdong Province (No. 20211216), the Medical Scientific Research Foundation of Guangdong Province (Nos. A2020096 and B2021330), the Research and Development Fund of Dongguan People's Hospital (No. k202005), the Guangdong medical university students' Innovation experiment program (Nos. 2021ZZDS006, 2021ZCDS003, 2022ZYDS003, 2022FYDB009, and

https://doi.org/10.1021/acsomega.3c01683
ACS Omega 2023, 8, 25066−25080

2022FCDS003), the Guangdong medical university students' Innovation and entrepreneurship training program (GDMU2021003, GDMU2021049, GDMU2022031, GDMU2022047, GDMU2022063, GDMU2022077, and GDMU2022078), the Provincial and national college students' innovation and entrepreneurship training program (Nos. 202210571008, S202210571075, S202110571078, and 202110571010), the Scientific Research Fund of Guangdong Medical University (No. GDMUZ2020009), the Guangdong Medical University—Southern Medical University twinning research team project (No. 4SG23033G), and the Cai Limin National Traditional Chinese Medicine Inheritance Studio.

REFERENCES

(1) Tezel, G.; Timur, S. S.; Bozkurt, I.; Türkoğlu, Ö. F.; Eroğlu, I.; Nemutlu, E.; öner, L.; Eroğlu, H. A Snapshot on the Current Status of Alzheimer's Disease, Treatment Perspectives, *in-Vitro* and *in-Vivo* Research Studies and Future Opportunities. *Chem. Pharm. Bull.* **2019**, *67*, 1030−1041.

(2) Yeung, C. H. C.; Lau, K.; Au, Y. S.; Schooling, C. M. Amyloid, tau and risk of Alzheimer's disease: A Mendelian randomization study. *Eur. J. Epidemiol.* **2021**, *36*, 81−88.

(3) Yang, J.; Zhao, J.; Tian, H.; Ren, J.; Wang, Z.; Liu, H.; Li, Z.Application of the theory of "mutual praise of spleen and kidney" in thetreatment of Alzheimers disease *Modernization of Traditional Chinese Medicine and Materia Medica-World Science and Technology* 2020; Vol. *22* 08, pp 2607−2614 DOI: 10.11842/wst.20200304002.

(4) Guan, X. Related theory of "five internal organs causing stupor" *Chin. J. Gerontol. 2015* 8 DOI: 10.3969/j.issn.1005-9202.2019.08.071.

(5) Ying, X. Analysis of Chemical Components and Material Basis for Neuroprotective Effect of Ershiwuwei Shanhu Pill. Ph.D. Thesis, Nankai University: Tianjin, CHN, 2014.

(6) Li, M. A Safety Evaluation and a Concomitant Toxicokinetics Study of Tibetan Medicine:25-ingredient Coral Pills. Master's Thesis; Chengdu University of Traditional Chinese Medicine: Chendu, CHN, 2011. https://cdmd.cnki.com.cn/Article/CDMD-10055-1015528882.htm.

(7) Hou, J.; Wang, C.; Zhang, M.; Ren, M.; Yang, G.; Qu, Z.; Hu, Y. Safflower yellow improves the synaptic structural plasticity by ameliorating the disorder of glutamate circulation in abeta(1-42)-induced AD model rats. *Neurochem. Res.* **2020**, *45*, 1870−1887.

(8) Xin, H. Separation and Identification of Carthamin Andits Protective Effect on Neuronal Injury Induced by Okadaic Acid in Differentiated SH-SY5Y Cells. Master's Thesis; Yantai University: Yantai, CHN, 2017 DOI: 10.7666/d.D01268222.

(9) Hu, X. D. A network pharmacology study on mechanism of Tibetan medicine Byur d Mar Nyer INga Ril Buagainst Alzheimer's disease. *Chin. Pharmacol. Bull.* **2019**, *35*, 128−132.

(10) Ying, X.; Liu, M.; Liang, Q.; Jiang, M.; Wang, Y.; Huang, F.; Xie, Y.; Shao, J.; Bai, G.; Luo, G. Identification and analysis of absorbed components and their metabolites in rat plasma and tissues after oral administration of 'Ershiwuwei Shanhu' pill extracts by UPLC-DAD/Q-TOF-MS. *J. Ethnopharmacol.* **2013**, *150*, 324−338.

(11) Ru, J.; Li, P.; Wang, J.; Zhou, W.; Li, B.; Huang, C.; Li, P.; Guo, Z.; Tao, W.; Yang, Y.; Xu, X.; Li, Y.; Wang, Y.; Yang, L. TCMSP: A database of systems pharmacology for drug discovery from herbal medicines. *J. Cheminf.* **2014**, *6*, 13.

(12) Butina, D.; Segall, M. D.; Frankcombe, K. Predicting ADME properties in silico: Methods and models. *Drug Discovery Today* **2002**, *7*, S83−S88.

(13) Li, L.; Li, Y.; Wang, Y. Prediction of BBB permeation based on molecular indices. *Chin. J. Med. Chem.* **2007**, *17*, 221.

(14) Kim, S.; Chen, J.; Cheng, T.; Gindulyte, A.; He, J.; He, S.; Li, Q.; Shoemaker, B. A.; Thiessen, P. A.; Yu, B.; Zaslavsky, L.; Zhang, J.; Bolton, E. E. PubChem 2023 update. *Nucleic Acids Res.* **2023**, *51*, D1373−D1380.

(15) Irwin, J. J.; Sterling, T.; Mysinger, M. M.; Bolstad, E. S.; Coleman, R. G. ZINC: A free tool to discover chemistry for biology. *J. Chem. Inf. Model.* **2012**, *52*, 1757−1768.

(16) Daina, A.; Michielin, O.; Zoete, V. SwissTargetPrediction: Updated data and new features for efficient prediction of protein targets of small molecules. *Nucleic Acids Res.* **2019**, *47*, W357−W364.

(17) Szklarczyk, D.; Morris, J. H.; Cook, H.; Kuhn, M.; Wyder, S.; Simonovic, M.; Santos, A.; Doncheva, N. T.; Roth, A.; Bork, P.; Jensen, L. J.; von Mering, C. The STRING database in 2017: Quality-controlled protein-protein association networks, made broadly accessible. *Nucleic Acids Res.* **2017**, *45*, D362−D368.

(18) Zhou, Y.; Zhou, B.; Pache, L.; Chang, M.; Khodabakhshi, A. H.; Tanaseichuk, O.; Benner, C.; Chanda, S. K. Metascape provides a biologist-oriented resource for the analysis of systems-level datasets. *Nat. Commun.* **2019**, *10*, No. 1523.

(19) Wang, Z.; Sun, H.; Yao, X.; Li, D.; Xu, L.; Li, Y.; Tian, S.; Hou, T. Comprehensive evaluation of ten docking programs on a diverse set of protein-ligand complexes: The prediction accuracy of sampling power and scoring power. *Phys. Chem. Chem. Phys.* **2016**, *18*, 12964−12975.

(20) Shen, Y.; Zhang, B.; Pang, X.; Yang, R.; Chen, M.; Zhao, J.; Wang, J.; Wang, Z.; Yu, Z.; Wang, Y.; Li, L.; Liu, A.; Du, G. Network Pharmacology-Based analysis of Xiao-Xu-Ming decoction on the treatment of alzheimer's disease. *Front Pharmacol.* **2020**, *11*, No. 595254.

(21) Zeng, P.; Wang, X. M.; Ye, C. Y.; Su, H. F.; Tian, Q. The main alkaloids in *uncaria rhynchophylla* and their Anti-Alzheimer's disease mechanism determined by a network pharmacology approach. *Int. J. Mol. Sci.* **2021**, *22*, No. 3612.

(22) Salvadó, G.; Mila-Aloma, M.; Shekari, M.; Minguillon, C.; Fauria, K.; Ninerola-Baizan, A.; Perissinotti, A.; Kollmorgen, G.; Buckley, C.; Farrar, G.; Zetterberg, H.; Blennow, K.; Suarez-Calvet, M.; Molinuevo, J. L.; Gispert, J. D. Cerebral amyloid-beta load is associated with neurodegeneration and gliosis: Mediation by p-tau and interactions with risk factors early in the Alzheimer's continuum. *Alzheimer's Dementia* **2021**, *17*, 788−800.

(23) Zhu, C. C.; Fu, S. Y.; Chen, Y. X.; Li, L.; Mao, R. L.; Wang, J. Z.; Liu, R.; Liu, Y.; Wang, X. C. Advances in Drug Therapy for Alzheimer's Disease. *Curr. Med. Sci.* **2020**, *40*, 999−1008.

(24) Tao, Z.; Lei, Z.; Rui, Z.; Gui-Hong, Y.; Hong-Bin, H.; De-Hua, C. Novel Mechanisms of Some Traditional Chinese Medicine for the Therapy of Neurocognitive Disorders. *Progress Biochem. Biophys.* **2020**, *47*, 729−742.

(25) Zhu, Y.; Zhu, W.; Li, L.; Liu, G.; Li, X.; Huang, C.; Tan, J.Clinical Observation on the Treatment of 30 Cases of Cerebral lnfarction with Ershiwuwei Shanhu Pill *Chin. J. Ethnomed. Ethnopharm.* 2020; Vol. *29* 09, pp 118−122 CNKI:SUN:MZMJ.0.2020-09-031.

(26) Jiao, J.; Zhong, G.; Li, H.; Hu, X.; Han, Y.; Chen, Q.; Wu, J.; Yin, H.Regulation of 25 Coral Pills on Intestinal Flora in Mice with Alzheimer's Disease *Modernization of Traditional Chinese Medicine and Materia Medica-World Science and Technology* 2022; Vol. *24* 01, pp 158−167 DOI: 10.11842/wst.20210604005.

(27) Gu, X. H.; Xu, L. J.; Liu, Z. Q.; Wei, B.; Yang, Y. J.; Xu, G. G.; Yin, X. P.; Wang, W. The Flavonoid Baicalein Rescues Synaptic Plasticity and Memory Deficits in a Mouse Model of Alzheimer's Disease. *Behav. Brain Res.* **2016**, *311*, 309−321.

(28) Wang, J.; Bo, Q.; Gong, J.; Cong, H.; Zhang, H.; Dong, H.Effects of Tenuigenin and *β*-asarone on AD Cells Model in Akt /GSK-3*β*s Signaling Pathway *Chin. Archives of Traditional Chin. Med.* 2018; Vol. *36* 04, pp 838−842 DOI: 10.13193/j.issn.1673-7717.2018.04.018.

(29) Wang, J.; Cui, L.; Zhang, Y.Interactions of amyloid precursor protein(APP) and its biological significance *Chin. Bull. Life Sci.* 2009; Vol. *21* 02, pp 253−258 DOI: 10.13376/j.cbls/2009.02.007.

(30) Chen, M.; Lu, L.; Luo, H.Research progress of amyloid *β*-protein in Alzheimer's disease *Chin. J. Gerontology* 2007, 11, pp 1112−1115 DOI: 10.3969/j.issn.1005-9202.2007.11.053.

https://doi.org/10.1021/acsomega.3c01683
ACS Omega 2023, 8, 25066−25080

(31) Zhang, X.; Zhang, L.; Yu, Y.Research progress of animal models of Alzheimer's disease *Lab. Animal Sci.* 2016; Vol. 33 05, pp 68−70 DOI: 10.3969/j.issn.1006-6179.2016.05.014.
(32) Jiao, Y.; Fang, J.; Zhuo, L.; Li, W.Mechanism of Huangkui Capsules in the Treatment of Diabetic Nephropathy Based on Network Pharmacology and Molecular Docking *World Chin. Med.* 2022; Vol. *17* 09, pp 1259−1264 DOI: 10.3969/j.issn.1673-7202.2022.09.011.
(33) Ma, M.; Cui, W.; Wang, B.; Li, Y.; Zhang, W.Expression of PIK3CA protein and PTEN protein in diffuse large B-cell Lymphoma and itsclinicopathological significance *J. Xinjiang Med. Univ.* 2022; Vol. *45* 01, pp 44−49 DOI: 10.3639/j.issn.1009-5551.2022.01.008.
(34) Ksiezak-Reding, H.; Pyo, H. K.; Feinstein, B.; Pasinetti, G. M. Akt/PKB kinase phosphorylates separately Thr212 and Ser214 of tau protein in vitro. *Biochim. Biophys. Acta* **2003**, *1639*, 159−168.
(35) Ahmad, F.; Singh, K.; Das, D.; Gowaikar, R.; Shaw, E.; Ramachandran, A.; Rupanagudi, K. V.; Kommaddi, R. P.; Bennett, D. A.; Ravindranath, V. Reactive oxygen species-mediated loss of synaptic akt1 signaling leads to deficient Activity-Dependent protein translation early in alzheimer's disease. *Antioxid. Redox Signaling* **2017**, *27*, 1269−1280.
(36) Vanhaesebroeck, B.; Guillermet-Guibert, J.; Graupera, M.; Bilanges, B. The emerging mechanisms of isoform-specific PI3K signalling. *Nat. Rev. Mol. Cell Biol.* **2010**, *11*, 329−341.
(37) Ye, L.; Wang, X.; Cai, C.; Zeng, S.; Bai, J.; Guo, K.; Fang, M.; Hu, J.; Liu, H.; Zhu, L.; Liu, F.; Wang, D.; Hu, Y.; Pan, S.; Li, X.; Lin, L.; Lin, Z. FGF21 promotes functional recovery after hypoxic-ischemic brain injury in neonatal rats by activating the PI3K/Akt signaling pathway via FGFR1/beta-klotho. *Exp. Neurol.* **2019**, *317*, 34−50.
(38) Howes, A. L.; Arthur, J. F.; Zhang, T.; Miyamoto, S.; Adams, J. W.; Dorn, G. N.; Woodcock, E. A.; Brown, J. H. Akt-mediated cardiomyocyte survival pathways are compromised by G alpha q-induced phosphoinositide 4,5-bisphosphate depletion. *J. Biol. Chem.* **2003**, *278*, 40343−40351.
(39) Razani, E.; Pourbagheri-Sigaroodi, A.; Safaroghli-Azar, A.; Zoghi, A.; Shanaki-Bavarsad, M.; Bashash, D. The PI3K/Akt signaling axis in Alzheimer's disease: A valuable target to stimulate or suppress? *Cell Stress Chaperones* **2021**, *26*, 871−887.
(40) Chu, F.; Li, K.; Li, X.; Xu, L.; Huang, J.; Yang, Z. Graphene oxide ameliorates the cognitive impairment through inhibiting PI3K/Akt/mTOR pathway to induce autophagy in AD mouse model. *Neurochem. Res.* **2021**, *46*, 309−325.
(41) Heras-Sandoval, D.; Perez-Rojas, J. M.; Hernandez-Damian, J.; Pedraza-Chaverri, J. The role of PI3K/AKT/mTOR pathway in the modulation of autophagy and the clearance of protein aggregates in neurodegeneration. *Cell. Signalling* **2014**, *26*, 2694−2701.
(42) O' Neill, C. PI3-kinase/Akt/mTOR signaling: Impaired on/off switches in aging, cognitive decline and Alzheimer's disease. *Exp. Gerontol.* **2013**, *48*, 647−653.
(43) Wani, A.; Gupta, M.; Ahmad, M.; Shah, A. M.; Ahsan, A. U.; Qazi, P. H.; Malik, F.; Singh, G.; Sharma, P. R.; Kaddoumi, A.; Bharate, S. B.; Vishwakarma, R. A.; Kumar, A. Alborixin clears amyloid-beta by inducing autophagy through PTEN-mediated inhibition of the AKT pathway. *Autophagy* **2019**, *15*, 1810−1828.
(44) Wang, C.; Zhang, X.; Teng, Z.; Zhang, T.; Li, Y. Down-regulation of PI3K/Akt/mTOR signaling pathway in curcumin-induced autophagy in APP/PS1 double transgenic mice. *Eur. J. Pharmacol.* **2014**, *740*, 312−320.
(45) Qi, Y.; Dou, D. Q.; Jiang, H.; Zhang, B. B.; Qin, W. Y.; Kang, K.; Zhang, N.; Jia, D. Arctigenin attenuates learning and memory deficits through PI3k/Akt/GSK-3beta pathway reducing tau hyper-phosphorylation in Abeta-Induced AD mice. *Planta Med.* **2017**, *83*, 51−56.
(46) Huang, Y.; Mucke, L. Alzheimer mechanisms and therapeutic strategies. *Cell* **2012**, *148*, 1204−1222.
(47) Wei, Z. W.; Hu, W. H. The development of anti-neuro-inflammatory agents for the treatment of Alzheimer' s disease. *Chin. Sci. Bull.* **2014**, *59*, 232−237.
(48) Ozben, T.; Ozben, S. Neuro-inflammation and anti-inflammatory treatment options for Alzheimer's disease. *Clin. Biochem.* **2019**, *72*, 87−89.
(49) Kumar, M.; Bansal, N. Implications of phosphoinositide 3-Kinase-Akt (PI3K-Akt) pathway in the pathogenesis of alzheimer's disease. *Mol. Neurobiol.* **2022**, *59*, 354−385.
(50) Chen, W.; Wu, L.; Hu, Y.; Jiang, L.; Liang, N.; Chen, J.; Qin, H.; Tang, N. MicroRNA-107 ameliorates damage in a cell model of alzheimer's disease by mediating the FGF7/FGFR2/PI3K/Akt pathway. *J. Mol. Neurosci.* **2020**, *70*, 1589−1597.
(51) Fan, L.; Qiu, X. X.; Zhu, Z. Y.; Lv, J. L.; Lu, J.; Mao, F.; Zhu, J.; Wang, J. Y.; Guan, X. W.; Chen, J.; Ren, J.; Ye, J. M.; Zhao, Y. H.; Li, J.; Shen, X. Nitazoxanide, an anti-parasitic drug, efficiently ameliorates learning and memory impairments in AD model mice. *Acta Pharmacol. Sin.* **2019**, *40*, 1279−1291.
(52) Ge, Q.; Wang, Z.; Wu, Y.; Huo, Q.; Qian, Z.; Tian, Z.; Ren, W.; Zhang, X.; Han, J. High salt diet impairs memory-related synaptic plasticity via increased oxidative stress and suppressed synaptic protein expression. *Mol. Nutr. Food Res.* **2017**, *61*, No. 1700134.
(53) Fang, W.; Bi, D.; Zheng, R.; Cai, N.; Xu, H.; Zhou, R.; Lu, J.; Wan, M.; Xu, X. Identification and activation of TLR4-mediated signalling pathways by alginate-derived guluronate oligosaccharide in RAW264.7 macrophages. *Sci. Rep.* **2017**, *7*, No. 1663.
(54) Yi, J.; Chen, B.; Yao, X.; Lei, Y.; Ou, F.; Huang, F. Upregulation of the lncRNA MEG3 improves cognitive impairment, alleviates neuronal damage, and inhibits activation of astrocytes in hippocampus tissues in Alzheimer's disease through inactivating the PI3K/Akt signaling pathway. *J. Cell. Biochem.* **2019**, *120*, 18053−18065.
(55) Liu, Y.; Song, X.; Zheng, S.; Luo, Y.; Wang, L.; Huang, F.; Qiu, X. Drug-Loaded nanoparticles from 'Ershiwuwei shanhu' pill induced cellular swelling of SH-SY5Y neuroblastoma cells. *J. Nanosci. Nanotechnol.* **2016**, *16*, 2336−2342.
(56) Nandi, A.; Yan, L. J.; Jana, C. K.; Das, N. Role of catalase in oxidative stress-and Age-Associated degenerative diseases. *Oxid. Med. Cell. Longevity* **2019**, *2019*, No. 9613090.
(57) Chen, Z.; Zhong, C. Oxidative stress in Alzheimer's disease. *Neurosci. Bull.* **2014**, *30*, 271−281.
(58) Ren, Z.; Dong, Z.; Xie, P.; Lv, J.; Hu, Y.; Guan, Z.; Zhang, C.; Yu, W. PNU282987 inhibits amyloid-beta aggregation by upregulating astrocytic endogenous alphaB-crystallin and HSP-70 via regulation of the alpha7AChR, PI3K/Akt/HSF-1 signaling axis. *Mol. Med. Rep.* **2020**, *22*, 201−208.
(59) Du, W.; Zhen, L.; Huang, F.; Li, P.; Shao, J.; Luo, Y.; Liu, Y.; Shang, Y.Effect of Ershiwuwei Shanhu Pill on NO and NOS in Plasma of Migraine Rats. Pharmacology and Clinics of Chinese Materia *Medica* 2013; Vol. *29* 02, pp 147−149 DOI: 10.13412/j.cnki.zyyl.2013.02.053.
(60) Fiaz, T.; Perveen, S.; Fatima, N. Study of complexation of dopamine analogues with bioactive metals by cyclic voltammetry. *J. Iran. Chem. Soc.* **2019**, *16*, 2211−2220.
(61) Folch, J.; Patraca, I.; Martinez, N.; Pedros, I.; Petrov, D.; Ettcheto, M.; Abad, S.; Marin, M.; Beas-Zarate, C.; Camins, A. The role of leptin in the sporadic form of Alzheimer's disease. Interactions with the adipokines amylin, ghrelin and the pituitary hormone prolactin. *Life Sci.* **2015**, *140*, 19−28.
(62) Li, S. T.; Dai, Q.; Zhang, S. X.; Liu, Y. J.; Yu, Q. Q.; Tan, F.; Lu, S. H.; Wang, Q.; Chen, J. W.; Huang, H. Q.; Liu, P. Q.; Li, M. Ulinastatin attenuates LPS-induced inflammation in mouse macrophage RAW264.7 cells by inhibiting the JNK/NF-kappaB signaling pathway and activating the PI3K/Akt/Nrf2 pathway. *Acta Pharmacol. Sin.* **2018**, *39*, 1294−1304.
(63) Hemonnot, A. L.; Hua, J.; Ulmann, L.; Hirbec, H. Microglia in alzheimer disease: Well-Known targets and new opportunities. *Front. Aging Neurosci.* **2019**, *11*, 233.

https://doi.org/10.1021/acsomega.3c01683
ACS Omega 2023, 8, 25066−25080